IFIC/16-48

Quasi-Dirac neutrinos at the LHC

G. Anamiati* and M. Hirsch†
AHEP Group, Instituto de Física Corpuscular – C.S.I.C./Universitat de València
Edificio Institutos de Investigacion, Parc Cientific de
Paterna, Apartado 22085, E–46071 València, Spain

E. Nardi‡
INFN, Laboratori Nazionali di Frascati
Via Enrico Fermi 40, 00044 Frascati, Italy

arXiv:1607.05641v2 [hep-ph] 28 Oct 2016

Abstract

Lepton number violation is searched for at the LHC using same-sign leptons plus jets. The standard lore is that the ratio of same-sign lepton to opposite-sign lepton events, R_{ll}, is equal to $R_{ll} = 1$ ($R_{ll} = 0$) for Majorana (Dirac) neutrinos. We clarify under which conditions the ratio R_{ll} can assume values different from 0 and 1, and we argue that the precise value $0 < R_{ll} < 1$ is controlled by the mass splitting versus the width of the quasi-Dirac resonances. A measurement of $R_{ll} \neq 0, 1$ would then contain valuable information about the origin of neutrino masses. We consider as an example the inverse seesaw mechanism in a left-right symmetric scenario, which is phenomenologically particularly interesting since all the heavy states in the high energy completion of the model could be within experimental reach. A prediction of this scenario is a correlation between the values of R_{ll} and the ratio between the rates for heavy neutrino decays into standard model gauge bosons, and into three body final states ljj mediated by off-shell W_R exchange.

Keywords: Neutrino mass, Lepton number violation, Inverse seesaw mechanism

*Electronic address: anamiati@ific.uv.es
†Electronic address: mahirsch@ific.uv.es
‡Electronic address: enrico.nardi@lnf.infn.it

Contents

I. Introduction 2

II. The inverse seesaw 4
A. Setup 5
B. Stepwise approximate diagonalization 6
C. Couplings to the gauge bosons and to the Higgs 7
D. A useful parametrization of the inverse seesaw in LR models 9

III. Opposite sign to same sign dilepton ratio 10

IV. LHC Phenomenology 12

V. Summary 17

Acknowledgments 18

References 18

I. INTRODUCTION

The tiny values of the standard model (SM) neutrino masses can be more elegantly explained under the assumption that neutrinos are Majorana particles. Majorana neutrinos necessarily imply lepton number violation (LNV), a well known LNV process is for example neutrinoless double beta decay (for reviews on $0\nu\beta\beta$ see for example [1, 2]). LNV is also searched for at the LHC, using as a signature final states containing two same-sign (SS) leptons (plus jets and no missing energy in the event). This signature, specific for collider searches, was originally proposed in [3] in the context of left-right (LR) symmetric extensions of the standard model (SM) [4–6].[1]

A heavy Majorana neutrino, once produced on mass-shell, decays with equal probabilities to either a lepton (l^-) or an anti-lepton (l^+) (plus, for example, jets). Therefore, for dilepton events produced via $W \to lN \to lljj$ a ratio of SS to opposite sign (OS) dileptons $R_{ll} = 1$ is expected.[2] For a Dirac neutrino $R_{ll} = 0$ since lepton number is conserved. In this paper we point out that in models with so-called "quasi-Dirac" neutrinos, R_{ll} can instead assume any value in the interval [0,1]. Hence a measurement of R_{ll}, different from zero or one, would provide valuable informations on the mechanism underlying the generation of

[1] Although it is not widely known, SS dilepton events are not a distinctive feature of LR scenarios. They can also arise, in principle, in a variety of LNV models [7] some of which do not introduce right-handed neutrinos.

[2] Via loop corrections small departures from exact $R_{ll} \equiv 1$ are possible. This signals CP violation and is a necessary ingredient for models of leptogenesis [8] (see [9–11] for reviews).

neutrino masses. Let us recall that "quasi-Dirac" refers to a pair of Majorana neutrinos with a small mass splitting and a relative CP-sign between the two states, and that would correspond to a Dirac neutrino in the limit of exact mass degeneracy. Pairs of quasi-Dirac neutrino often appear in seesaw-type models at scales not far from the electroweak scale, such as the inverse [12] and the linear [13, 14] seesaw, so that the possibility of observing $R_{ll} \neq 1, 0$ is naturally interweaved with the possibility of producing new heavy neutrinos in high energy collisions.[3]

Both, the ATLAS [17, 18] and the CMS collaboration [19, 20] have published results for dilepton plus jets $\ell\ell jj$ events. In general, the sensitivities of ATLAS and CMS are quite similar. Nevertheless, there are some important differences in the analysis of the two collaborations. ATLAS, in its first publication [17], gave results for both, SS and OS lepton events separately. Since no excess was observed and the background in the OS sample is considerably larger than in the SS sample, the limits derived from the combined data are dominated by the SS sample. Note that this combination assumes implicitly $R_{ll} = 1$. Probably for this reason, in the latest analysis [18] ATLAS gives only the limits derived from the SS sample. CMS, on the other hand, gives only combined results for OS and SS samples [19, 20], despite the fact that CMS routinely measures the lepton charge. In the latest CMS analysis, which uses the full $\sqrt{s} = 8$ TeV statistics [20], an excess in the electron sample around $m_{eejj} \simeq 2$ TeV was reported. The excess contains 14 events with an estimated background of 4 events, corresponding to a local significance of about 2.8 σ c.l. No excess was observed in the muon sample. CMS points out that (i) only one of the 14 events is SS and (ii) no localized excess in $m_{\ell_2 jj}$, as would be expected from the decay of an on-shell intermediate N, is observed, and thus it was concluded that the excess is not consistent with the expectations from LR symmetric models. ATLAS, on the other hand, has zero events in the same invariant mass bin, but since in [18] ATLAS does not provide results for OS dileptons, their result is not inconsistent with CMS. The CMS excess has caused a flurry of theoretical activity [21], several of the proposed explanations are based on LR symmetric models, see for example the works in [22–26], where however $R_{ll} = 1$ is generally expected. Note that $R_{ll} = 0$ is expected in LR models with a linear seesaw [27], while $R_{ll} < 1$ can be obtained in the R-parity violating supersymmetric model of [28]. However, particularly relevant for our study is [29] which also focuses on a LR symmetric model equipped with the inverse seesaw mechanism, and where it is stressed that heavy pseudo-Dirac neutrinos allow to arrange for a suppression of SS versus OS dilepton events, and hence for a value of $R_{ll} < 1$. Although we agree on the general statement, we find disagreement as concerns the dependence of R_{ll} on the relevant model parameters. In particular, differently from [29], we find that the value of R_{ll} does not display a parametric dependence on the overall right-handed (RH) neutrino mass scale.[4]

[3] Scenarios with quasi degenerate right-handed neutrinos with masses and couplings allowing for their production at the LHC, but of the Dirac type [15], or effectively yielding lepton number conservation [16], have been also proposed.

[4] The authors of [30] study the inverse seesaw within the standard model group. We agree with their

Neutrino oscillation experiments have established that neutrino flavor numbers are not conserved. By now we have very precise information on the active neutrino mixing angles, see for example [31]. Basically the "solar", $\sin^2\theta_\odot \simeq 1/3$, and "atmospheric", $\sin^2\theta_{\rm Atm} \simeq 1/2$, angles are large, while the "reactor" angle, $\sin^2\theta_{\rm R} \simeq 0.0234$, is smaller. It is therefore quite unnatural to assume that heavy neutrinos, if they exist, would only decay to the same lepton flavor associated with their production (as for example in $W_R^+ \to \ell_j^+ N_R \to \ell_j^+ \ell_j^- W_R^*$). From the theoretical point of view, different flavor dilepton events $\ell_i^+\ell_j^-$ and $\ell_i^+\ell_j^+$ with $i \neq j$ are expected to contribute sizeably to the whole dilepton samples, and for some choices of the model parameters they could even dominate the total signal. The relative amount of different flavor dilepton events could also provide valuable information about the structure of the seesaw matrices. Unfortunately, both ATLAS and CMS use $e\mu$ dilepton samples to estimate the backgrounds, giving results only for ee and $\mu\mu$ samples separately. We would like to stress that different flavor dilepton events should also be considered as a possible signal, and that presenting experimental results separately for each specific flavor channel would provide additional valuable information.

This paper is organized as follows. In the next section, we recall the main features of the inverse seesaw model [12], we describe in some details the steps to achieve approximate diagonalization of the full 9×9 neutrino mass matrix, and we write down the heavy neutrino couplings to the LR gauge bosons and to the Higgs. In the same section we also introduce a convenient parametrization which, in the inverse seesaw, plays an analogous role as the Casas-Ibarra parametrization [32] in the type-I seesaw. In section III we derive the expression for the ratio R_{ll}. Our result shows that the condition required for obtaining values of $R_{ll} \neq 0, 1$ is that the mass degeneracy of the quasi-Dirac neutrino pairs must be of the order of their decay width. In section IV we discuss all relevant phenomenology (two and three body decays and branching ratios) that could be measured at the LHC. We close with a short summary.

II. THE INVERSE SEESAW

In this section we discuss the inverse seesaw mechanism. In subsection II A we present the inverse seesaw mass matrix and parameter counting, in II B we describe an approximate diagonalization procedure for the 9×9 mass matrix, in II C we give the neutrino couplings to gauge (and Higgs) bosons, and in II D we provide a re-parametrization of the inverse seesaw that allows to fulfill automatically the experimental constraints from low-energy neutrino data. While we are mostly interested in a LR symmetric setup with a gauge group $SU(3)_C \times SU(2)_L \times SU(2)_R \times U(1)_{B-L}$, most of the discussion in this section applies also to inverse seesaw within the SM. We will formulate this section in the LR context and we

expression for the LNV amplitude. However, different from the LR case, which we study in this paper, [30] concludes that LNV events are not observable for heavy neutrino masses above 100 GeV in their setup.

will comment on differences between inverse seesaw within the LR symmetric and the SM scenarios at the end of the section.

A. Setup

We work in the basis in which the mass matrix of the charged lepton is diagonal, with the e, μ, τ flavors identified by the mass eigenvalues. We write the inverse seesaw mass matrix in the interaction basis for the neutral states $\mathcal{N} = (\nu_L, N_R^c, S_R^c)^T$ where $\nu_L = (\nu_e, \nu_\mu, \nu_\tau)^T$ is the vector of the $SU(2)$ partners of the LH charged leptons containing the (mainly light eigenstate) LH neutrinos, $N_R = (N_e, N_\mu, N_\tau)^T$ is the vector of the neutral member of the $SU(2)_R$ doublets $\ell_R = (N_R, e_R)$, and $S_R = (S_1, S_2, S_3)^T$ is a vector of gauge singlet fermions for which a Majorana mass term $\mu \overline{S^c} S$ is allowed. In 3×3 block notation the mass matrix reads:

$$\mathcal{M} = \begin{pmatrix} 0 & m_D^T & 0 \\ m_D & 0 & M_R \\ 0 & M_R^T & \hat{\mu} \end{pmatrix} , \tag{1}$$

where the Majorana sub-matrix $\hat{\mu}$ (as well as the full $\mathcal{M}$) is complex symmetric. Any complex symmetric matrix m of any dimension can be factorized in a unique way as $m = W^* \hat{m} W^\dagger$ where $\hat{m}$ is diagonal with real and positive eigenvalues, and W is unitary. Then, by redefining the gauge singlets S via a unitary rotation $W(\mu)$ we can always bring μ into diagonal form $\hat{\mu}$ as is implicit in eq. (1). As regards M_R, if the fields N_R were unrelated to the SM leptons further field redefinitions would be possible. However, in the LR model the N_R's sit in the same $SU(2)_R$ multiplets with the RH SM leptons, and once a redefinition of ℓ_R (together with a redefinition of ℓ_L) is used to bring into diagonal form the charged lepton mass matrix, the only residual freedom is in three vectorlike phase redefinitions of $\ell_{L,R}$ proportional to the three diagonal $U(3)$ generators I, λ_3, λ_8 which commute with the diagonal mass matrix. This can be used to remove three phases from M_R which remains otherwise generic with $9 + 6$ (real + imaginary) parameters. Finally, because of LR symmetry in exchanging the L and R labels, the complex matrix m_D is symmetric.

Exact diagonalization of the mass matrix eq. (1) can be performed via a transformation of the field basis with a unitary matrix $\mathcal{V}$ such that

$$\hat{\mathcal{M}} = \mathcal{V}^T \mathcal{M} \mathcal{V} , \tag{2}$$

is diagonal. Of course, in the general case this can only be done numerically (our numerical study indeed relies on a precise numerical diagonalization of the full 9×9 matrix). However, assuming that the three sub-matrices in eq. (1) have mass scales arranged hierarchically μ, $m_D \ll M_R$, an approximate diagonalization can be performed in analytic form yielding:

$$\hat{\mathcal{M}}' = \mathcal{V}'^T \mathcal{M} \mathcal{V}' \approx \hat{\mathcal{M}} \tag{3}$$

where $\mathcal{V}' \approx \mathcal{V}$ is non-unitary by terms of $\mathcal{O}(m_D/M_R)$ (we denote with a prime non-unitary transformation matrices, as well as mass matrices obtained via non-unitary transformations).

Clearly $\hat{\mathcal{M}}'$ deviates from exact diagonal form: terms of $\mathcal{O}(\mu\, m_D/M_R)$ will appear in the non-diagonal entries coupling the light and heavy sectors, and terms of $\mathcal{O}(\mu)$ will appear in the non diagonal entries of the heavy sector. Below we give a brief description of this approximate diagonalization procedure, which will also be useful to establish notations.

B. Stepwise approximate diagonalization

Approximate diagonalization can be carried out in four steps. The first step is to bring M_R into diagonal form. Let us decompose M_R in terms of two unitary matrices U_R, V_R and a diagonal matrix of mass eigenvalues $\hat{M}_R$:

$$M_R = U_R \hat{M}_R V_R^\dagger \,. \tag{4}$$

As we have remarked above, M_R contains nine real and six imaginary parameters. Then, by matching the number of parameters between the LH and RH sides of eq. (4) we see that U_R and V_R can be taken as special unitary, with three real angles and three phases each. The matrix U_R is an important quantity since, for example, it will appear in the RH charged currents coupling N_R to the charged leptons. By defining a block-diagonal matrix $V_1 = \mathrm{diag}\,(\mathbb{I}_3, U_R^*, V_R)$, where $\mathbb{I}_3$ is the 3×3 identity matrix, it is easy too see that in the matrix $\mathcal{M}_1 = V_1^T \mathcal{M} V_1$ an exact diagonalization $M_R \to \hat{M}_R$ is obtained, while at the same time $\hat{\mu} \to \mu^V \equiv V_R^T \hat{\mu} V_R$ and the entries m_D (m_D^T) get replaced by D (D^T) defined as:

$$D \equiv U_R^\dagger m_D \,. \tag{5}$$

The next step $\mathcal{M}_2 = V_2^T \mathcal{M}_1 V_2$ with $V_2 = \frac{1}{\sqrt{2}}\mathrm{diag}(\sqrt{2}, \sigma_1 - \sigma_3) \otimes \mathbb{I}_3$ brings $\hat{M}_R$ to the block-diagonal (2,2) and (3,3) entries and also adds to these entries small corrections of $\mathcal{O}(\mu^V)$. The D terms eq. (5) remain in the first row $(\mathcal{M}_2)_{1j} = v_D^T = \frac{1}{\sqrt{2}}(0, -D^T, D^T)$ and first column $(\mathcal{M}_2)_{j1} = v_D$. Let us note that since V_1 and V_2 are both unitary, no approximation has been made so far in $\mathcal{M}_2$. The next step requires suppressing the off-diagonal entries of order m_D. This is obtained with a matrix V_3' such that $(V_3')_{1j} = w_D^\dagger = (\mathbb{I}_3, D^\dagger, D^\dagger)\frac{1}{\sqrt{2}\hat{M}_R}$, $(V_3')_{j1} = -w_D$ and $(V_3')_{jj} = \mathbb{I}_3$. It can be easily checked that $V_3' V_3'^\dagger$ deviates from the identity by $\mathcal{O}(m_D^2/M_R^2)$. With this rotation, the off-diagonal light-heavy entries in $\mathcal{M}_3' = V_3'^T \mathcal{M}_2 V_3'$ get suppressed to $\mathcal{O}(\hat{\mu} D/M_R^2)$ which, in the seesaw approximation, can be neglected. We have thus singled out in the (1,1) block the light neutrino mass matrix m_ν, which can now be expressed, as is customary, in terms of the initial matrices in eq. (1) as:

$$m_\nu \simeq m_D^T \frac{1}{M_R^T} \hat{\mu} \frac{1}{M_R} m_D \,. \tag{6}$$

We see from this equation that suppression of the light neutrino masses can be obtained thanks to small values of $\hat{\mu}$, without the need of exceedingly small values of m_D/M_R. This can allow for N_R to live at relatively low energy scales, possibly within experimental reach. Being symmetric by construction, m_ν can be diagonalized as

$$\hat{m}_\nu = {V_L}^T \, m_\nu \, V_L \,, \tag{7}$$

with V_L unitary. Note that V_L differs from the exact (non-unitary) light neutrinos mixing matrix V_L' by $\mathcal{O}(\frac{m_D}{M_R})$. In our study we will neglect these small terms and we will identify $V_L = V_L'$. A last rotation, by means of the unitary matrix $V_4 = \mathrm{diag}\,(V_L,\, i\,\mathbb{I}_3,\, \mathbb{I}_3)$, can now be performed on $\mathcal{M}_3'$ to bring m_ν into diagonal form (this also renders positive the heavy mass entries in the (2,2) block that have acquired a negative sign). Neglecting the small off-diagonal entries, the final matrix $\mathcal{M}' = V_4^T \mathcal{M}_3' V_4$ reads:

$$\mathcal{M}' \simeq \begin{pmatrix} \hat{m}_\nu & 0 & 0 \\ 0 & \hat{M}_R^- & 0 \\ 0 & 0 & \hat{M}_R^+ \end{pmatrix}. \tag{8}$$

The eigenvalues of the two 3×3 heavy-heavy blocks $\hat{M}_R^\pm$ receive corrections of $\mathcal{O}(m_D^2/\hat{M}_R)$ after the V_4 rotation. However, these corrections are the same for both blocks, so that they can be conventionally absorbed into a common term $\hat{M}_R$. Instead, contributions of order $\hat{\mu}$ appear with opposite sign, and this is important because it generates small splittings between pairs of heavy states. For our analysis it is then sufficient to define the heavy mass eigenvalues in eq. (8) as $\hat{M}_R^\pm = \hat{M}_R \pm \frac{1}{2}\mu^V$, keeping in mind that they represent three pairs of almost degenerate (quasi-Dirac) neutrinos with large masses $(\hat{M}_R)_{ii}$, split by three small quantities $(\Delta M)_{ii} = (\hat{M}_R^+)_{ii} - (\hat{M}_R^-)_{ii} = (\mu^V)_{ii}$ where $\mu^V \equiv V_R^T \hat{\mu} V_R^T$ (this last definition is given here for the sake of precision, but being V_R and $\hat{\mu}$ in any case arbitrary, in the following we will simply denote the mass splittings generically as $\Delta M = \mu$).

C. Couplings to the gauge bosons and to the Higgs

The approximate mixing matrix $\mathcal{V}' = V_1\, V_2\, V_3'\, V_4$ derived in the previous section controls the structure of the couplings between the LR gauge bosons and the mass eigenstates. Its explicit form is:

$$\mathcal{V}' = \begin{pmatrix} V_L & \frac{i}{\sqrt{2}}\xi^\dagger & \frac{1}{\sqrt{2}}\xi^\dagger \\ 0 & -\frac{i}{\sqrt{2}}U_R^* & \frac{1}{\sqrt{2}}U_R^* \\ -V_R\xi V_L & \frac{i}{\sqrt{2}}V_R & \frac{1}{\sqrt{2}}V_R \end{pmatrix} \tag{9}$$

where for convenience we have introduced the 3×3 matrix of small mixings:

$$\xi = \frac{1}{\hat{M}_R}\, D = \frac{1}{\hat{M}_R}\, U_R^\dagger\, m_D\,. \tag{10}$$

The derivation of the charged current (CC) couplings to $W_{L,R}^\pm$ and of the neutral current (NC) couplings to $Z_{L,R}$ is outlined below. It is left understood that the known SM couplings fix the normalization modulo a factor of the ratio of the gauge couplings g_R/g_L. Let us introduce a vector $E = (e_L, e_R^c, 0)^T$ for the left-handed (mass eigenstate) charged fermions, and recall that the neutral states are arranged in another vector $\mathcal{N} = (\nu_L, N_R^c, S_R^c)^T$. The

LH and RH charged currents can be written (in two component notations) as:

$$J_L^{-\mu} \;=\; \frac{1}{\sqrt{2}}\, E^\dagger \bar{\sigma}^\mu\, p_L\, \mathcal{N}\,, \tag{11}$$

$$J_R^{-\mu} \;=\; \frac{1}{\sqrt{2}}\, E^\dagger \bar{\sigma}^\mu\, p_R\, \mathcal{N}\,, \tag{12}$$

where $\bar{\sigma}^\mu = (1, -\vec{\sigma})$ are the spinor matrices, and $p_{L,R}$ are the projectors onto the neutral members of the L and R multiplets corresponding to 9×9 matrices which, in 3×3 block notation, are given by $(p_L)_{11} = \mathbb{I}_3$, $(p_R)_{22} = \mathbb{I}_3$ with zero in all other entries. In the seesaw approximation, the neutral mass eigenstates are related to the interaction eigenstates as $\mathcal{N} = \mathcal{V}'\, N$ with $N = (\nu, N_-, N_+)^T$, where ν represents the three light neutrinos and $N_\pm$ correspond to the heavy neutrinos respectively with mass eigenvalues $M_R^\pm$. Projecting onto the mass eigenstates and converting to the usual four-component spinor notation for gauge currents we have:

$$J_L^{-\mu} \;=\; \frac{1}{\sqrt{2}}\, \bar{e}_L \gamma^\mu\, V_L \nu + \frac{1}{2}\, \bar{e}_L \gamma^\mu\, \xi^\dagger\, (N_+ + i N_-)\,, \tag{13}$$

$$J_R^{-\mu} \;\sim\; \frac{1}{2}\, \overline{e_R^c}\, \gamma^\mu\, U_R^*\, (N_+ - i N_-)\,. \tag{14}$$

NC couplings are also important since they can give rise to $N_\pm \to Z\nu$ decays. In the interaction basis the NC for the neutral states are:

$$J_L^{0\mu} \;=\; \frac{1}{2} \mathcal{N}^\dagger i \bar{\sigma}^\mu\, p_L\, \mathcal{N}\,, \tag{15}$$

$$J_R^{0\mu} \;=\; \frac{1}{2} \mathcal{N}^\dagger i \bar{\sigma}^\mu\, p_R\, \mathcal{N}\,, \tag{16}$$

which in the mass eigenstate basis yields:

$$J_L^{0\mu} \;=\; \frac{1}{2} \bar{\nu} \gamma^\mu\, \nu + \frac{1}{2\sqrt{2}} \left[\bar{\nu} \gamma^\mu V_L^\dagger \xi^\dagger (N_+ + i N_-) + H.c. \right]\,, \tag{17}$$

$$J_R^{0\mu} \;=\; \frac{1}{4}\, (\bar{N}_+ + i \bar{N}_-) \gamma^\mu (N_+ - i N_-)\,. \tag{18}$$

In the first equation we have neglected additional terms involving N-N couplings which are suppressed as $\xi\xi^\dagger$. As can be seen from the second equation, in the approximation in which terms of order $\mu/\hat{M}_R \xi$ are neglected there are no R-handed neutral currents between heavy and light neutrinos. Finally, the fermion-scalar coupling $\frac{1}{v} N_R^\dagger m_D \nu_L\, H$ gives the following interactions between the heavy $N_\pm$'s, the Higgs and the light neutrinos:

$$\begin{aligned} \mathcal{L}_H \;=\; & \frac{1}{\sqrt{2}} (\bar{N}_+ + i \bar{N}_-) \left[U_R^T \frac{m_D}{v}\, V_L \right] \nu\, H \\ & +\; \frac{1}{2} (\bar{N}_+ + i \bar{N}_-) \left[U_R^T \frac{m_D}{v} \xi^\dagger \right] (N_+ + i N_-) H + H.c.\,. \end{aligned} \tag{19}$$

D. A useful parametrization of the inverse seesaw in LR models

In [32] a clever parametrization of the Dirac mass matrix of the type I seesaw was put forth, and it is referred to as the Casas-Ibarra (CI) parametrization. In this parametrization m_D is expressed in terms of low energy observables (light neutrino mass eigenvalues and mixing angles), of the seesaw heavy mass eigenvalues, and of an arbitrary complex orthogonal matrix $\mathcal{R}$. One of the most useful features of the CI parametrization is that it allows to generate random samples of m_D which by construction reproduce all the low energy data, which is a quite valuable property when one wants to scan over the model parameter space. As we detail below, also for the inverse seesaw in LR models it is possible to introduce a parametrization that has analogous properties, namely that allows to scan over the unknown physical masses and couplings (U_R, V_R, m_D, M_R, $\hat{\mu}$) while automatically reproducing all the low energy data.

Let us start by writing the light neutrino mass matrix in diagonal form (see eq. (6) and eq. (7)):

$$\hat{m}_\nu \;=\; V_L^T m_D^T \frac{1}{M_R^T} \hat{\mu} \frac{1}{M_R} m_D V_L \,. \tag{20}$$

Let us now write m_D as:

$$m_D \;=\; M_R \, \frac{1}{\sqrt{\hat{\mu}}} \, \mathcal{R} \, \sqrt{\hat{m}} \, V_L^\dagger \,. \tag{21}$$

By inserting eq. (21) into the RH side of eq. (20) (or by extracting directly $\mathcal{R}$ from eq. (21)) it can be verified that $\mathcal{R}$ must satisfy the condition $\mathcal{R}\mathcal{R}^T = \mathcal{R}^T\mathcal{R} = I$, but is otherwise arbitrary, and thus it can be written as a generic 3×3 orthogonal matrix in terms of three complex angles. Rewriting M_R in the previous equation according to eq. (4) we obtain

$$D = U_R^\dagger \, m_D = \hat{M}_R \, V_R^\dagger \, \frac{1}{\sqrt{\hat{\mu}}} \, \mathcal{R} \, \sqrt{\hat{m}} \, V_L^\dagger \,. \tag{22}$$

The RH side of this equation is written in terms of the low energy observables ($\sqrt{\hat{m}} \, V_L^\dagger$) while the other quantities are arbitrary. The crucial point now is to factor the generic 3×3 complex matrix D as defined in eq. (22) into a unitary matrix ($U_R^\dagger$) and a symmetric matrix (m_D). This can be achieved by factorizing D in its singular value decomposition (SVD) in terms of two unitary matrices W and Q and a real diagonal matrix with non-negative entries $\hat{D}$:

$$D = W \cdot \hat{D} \cdot Q^\dagger = (W Q^T) \cdot (Q^* \hat{D} Q^\dagger) \equiv \tilde{U}_R^\dagger \tilde{m}_D \,, \tag{23}$$

where, in the second step, we have inserted $Q^T Q^* = \mathbb{I}_3$ in order to build up a unitary matrix $\tilde{U}_R$ and the symmetric matrix $\tilde{m}_D$. However, $\tilde{U}_R$ and $\tilde{m}_D$ found in this way are just one among a threefold infinite class of possibilities, spanned by the freedom in switching phases between $\tilde{U}_R$ and $\tilde{m}_D$ (all the moduli are instead uniquely fixed). This is due to the fact that the SVD decomposition is not unique, since there are 9 phases in D and 12 in its

decomposition in terms of $W, \hat{D}$ and Q. However, as discussed below eq. (4), without loss of generality U_R can be taken special unitary with just 3 phases, and doing so the counting of parameters between the LH and RH sides of eq. (23) matches. Let us then introduce a diagonal matrix of phases $\Phi = \mathrm{diag}(e^{i\varphi_1}, e^{i\varphi_2}, e^{i\varphi_3})$ and make the identification

$$U_R = Q^* \Phi^* W^\dagger \,, \qquad m_D = Q^* \Phi^* \hat{D} Q^\dagger \,, \tag{24}$$

which clearly preserves $U_R^\dagger m_D = D$ and the symmetric nature of m_D. The values of φ_i can then be fixed to achieve the desired form for U_R. Therefore, in the LR inverse-seesaw, given for example a set of RH neutrino masses $\hat{M}_R$ and of LNV parameters $\hat{\mu}$ of specific interest, the parametrization eq. (23) together with eq. (24) yields both m_D and U_R in terms of two arbitrary matrices: a complex orthogonal matrix $\mathcal{R}$ and a special unitary matrix V_R with just three phases, while, by construction, all the low energy neutrino data are automatically reproduced.

The discussion in this section assumed an inverse seesaw within the left-right symmetric group. However, it is straightforward to adapt most our discussion to inverse seesaw models with the same block structure of $\mathcal{M}$ as in eq. (1), but for which N_R is not related to ℓ_R, i.e. the standard model gauge group. In this case m_D is not constrained to be symmetric and we gain the freedom of redefining N_R via a $U(3)$ transformation. This allows to reabsorb U_R defined in eq. (4) via a field rotation, while V_R remains defined in terms of three real and three imaginary parameters. Then $U_R^\dagger$ can be simply dropped from eq. (22) whereas $D = m_D$ remains generic. [5]

III. OPPOSITE SIGN TO SAME SIGN DILEPTON RATIO

In this section we estimate the ratio of production of pairs of leptons with the same sign and we compare it with the rate of production of pairs of leptons of opposite sign. The ratio between these two observables is denoted as R_{ll}. In both cases the production rates are dominated by processes with on-shell (or nearly on-shell) N_R's and therefore, under the natural assumption that the mass splitting between the different pairs is large (we typically expect $M_{Rj}^\pm - M_{Rk}^\pm \sim \mathcal{O}(M_R)$), it is sufficient to study just a single pair of quasi-Dirac $N_\pm$. SS dilepton production occurs for example through the LNV process $\bar{q}q \to W_R^+ \to \ell_\alpha^+ N_\pm \to \ell_\alpha^+ \ell_\beta^+ W_R^*$, where $(\bar{q})q$ denote (anti-)quark partons inside the colliding protons, N_+ and N_- are the two heavy neutrinos mass eigenstates, W_R^* is an off-shell RH gauge boson that will eventually decay dominantly in two jets, and ℓ_α, ℓ_β are two leptons not necessarily of the same flavor. Opposite sign pairs of leptons can be produced via the LN conserving process $\bar{q}q \to W_R^+ \to \ell_\alpha^+ N_\pm \to \ell_\alpha^+ \ell_\beta^- W_R^*$. Clearly, in order to produce the $N_\pm$ intermediate states on-shell via the decay of an on-shell W_R, $M_{W_R} > M_R^\pm$ is required. We further assume $M_{W_R} \not\gg M_R^\pm$ so that the $N_\pm$ mass eigenstates can be treated in the non-relativistic approximation.

[5] Of course, within the SM group there are no right-handed gauge interactions, see section II C.

Before entering into details let us try to figure out qualitatively what type of result we can expect. When the on-shell W_R^+ decays, an ℓ^+ anti-lepton is produced together with a heavy neutrino of ℓ-flavor N_ℓ, which corresponds to a coherent superposition of the two mass eigenstates $N^\pm$. Given that the same decay channels are open for both $N^\pm$, the time-evolution of the initial N_ℓ will be characterized by a typical oscillating behavior with frequency $\Delta M = M^+ - M^- = \mu$. There is another important scale in the problem, that is the $N^\pm$ lifetime $\tau = 1/\Gamma$.[6] If $\Delta M \gg \Gamma$ the lifetime is long enough that complete separation of the $N^\pm$ wave packets can occur. Coherence between the two mass eigenstates is completely lost before the decays, and decays will then proceed as in the usual Majorana case, yielding equal probabilities for SS and OS dileptons events, i.e. $R_{ll} = 1$. (Ideally, in this situation we can imagine that the mass of the intermediate state can be reconstructed from the invariant mass of the N decay products $m_{\ell_2 jj}$ to be M^+ or M^-, in which case the above result is obvious.) In the opposite limit $\Delta M \ll \Gamma$ decays occur at a time $t_D \sim \tau \ll 1/\Delta M$, that is before the onset of oscillation effects, so that $N_\ell(t_D) \approx N_\ell(0)$. In this case only the LN conserving transition $N_\ell(t_D) \to \ell^-$ can occur and $R_{ll} = 0$. Namely, when the $N^\pm$ mass degeneracy (in units of Γ) is sufficiently strong, the pure Dirac case is approached. It is then clear that the interesting regime occurs when the oscillation frequency is of the order of the lifetime, viz when $\mu = \Delta M \approx \Gamma$. Only in this case we can expect $R_{ll} \neq 0, 1$.

From eq. (9) we can write the N_ℓ heavy state produced in the decay $W_R^+ \to \bar{\ell} N_\ell$ and its conjugate state $N_{\bar{\ell}}$ produced in the decay $W_R^- \to \ell N_{\bar{\ell}}$ in terms of the mass eigenstates as:[7]

$$N_\ell = \frac{1}{\sqrt{2}}(N_+ - iN_-)\,, \tag{25}$$

$$N_{\bar{\ell}} = \frac{1}{\sqrt{2}}(N_+ + iN_-)\,. \tag{26}$$

In writing these linear combinations we have neglected for convenience the flavor mixing matrices U_R (see eq. (9)) since the products of their matrix elements appearing in the LN conserving and LNV amplitudes cancels in the ratio R_{ll}. However, it should be kept in mind that these matrix elements control the flavor composition of both the SS and OS dilepton final states $\ell_i \ell_j$, and we reiterate that for generic mixing structures, $i \neq j$ events have no reason to be suppressed with respect to $i = j$ events.

After a time t, the states in eq. (29) have evolved into [33]

$$N_\ell(t) = g_+(t) N_\ell + g_-(t) N_{\bar{\ell}}\,, \tag{27}$$

$$N_{\bar{\ell}}(t) = g_-(t) N_\ell + g_+(t) N_{\bar{\ell}}\,, \tag{28}$$

[6] Since $N^\pm$ have the same decay channels, and only a tiny mass difference, we expect for the width difference $\Delta\Gamma = \Gamma^+ - \Gamma^- \ll \Delta M$ so that $\Delta\Gamma$ is always negligible. This is analogous to what happens in the $B^0 - \bar{B}^0$ meson system (see e.g. ref. [33]).

[7] One remark is in order: in the presence of CP violating effects, the modulus of the ratio of the two coefficients in the linear combinations eqs. (25)–(26) can deviate from unity (CP violation in mixing [33]). In the regime $\mu \sim \Gamma$ this type of CP violation can get resonantly enhanced, and in principle observable effects on the ratio R_{ll} could be possible. We neglect this possibility in our treatment.

where the oscillating amplitudes read

$$g_+(t) \;=\; e^{-iMt}e^{-\frac{\Gamma}{2}t}\cos\left(\frac{\Delta M}{2}t\right)\,, \tag{29}$$

$$g_-(t) \;=\; i\,e^{-iMt}e^{-\frac{\Gamma}{2}t}\sin\left(\frac{\Delta M}{2}t\right)\,, \tag{30}$$

with $M=\frac{1}{2}(M_+ + M_-)$ and, according to the discussion above, we have neglected the effects of $\Delta\Gamma$. Since the typical heavy neutrino widths are too large to allow observing displaced vertices (see next section), individual oscillation patterns cannot be resolved. The SS to OS ratio R_{ll} is then given by the ratio of the time-integrated amplitudes squared (note that they include the time dependent weight factor of the heavy neutrinos lifetime):

$$R_{ll} = \frac{\int_0^\infty |g_-|^2\,dt}{\int_0^\infty |g_+|^2\,dt} = \frac{\Delta M^2}{2\Gamma^2+\Delta M^2}\,. \tag{31}$$

This result correctly reproduces the limiting cases discussed at the beginning of this section, that is $R_{ll}\to 1$ as $\Gamma/\Delta M\to 0$ (limiting Majorana case) and $R_{ll}\to 0$ as $(\Gamma/\Delta M)^{-1}\to 0$ (limiting Dirac case).[8]

IV. LHC PHENOMENOLOGY

In searching for heavy RH neutrinos within the framework of LR symmetric models, both the ATLAS [17, 18] and the CMS collaboration [19, 20] assume that the heavy neutrino decays proceed via an off-shell W_R bosons, with a branching ratio of 100% for the decay mode $N\to l^\pm jj$ where l represents a charged lepton of any flavor and N represents a generic heavy neutrino. While this is a reasonable expectation for LR models with an ordinary seesaw mechanism, the situation is very different in models based on the inverse seesaw. In our framework in fact all the following decay modes can occur, and all with sizeable branching ratios:

$$\begin{gathered} N\to W_L^\pm + l^\pm\,,\quad N\to Z_L+\nu\,,\quad N\to h+\nu\,, \\ N\to (W_R)^* + l^\pm \to jjl^\pm\;,\; N\to (Z_R)^*+\nu\to (jj \text{ or } l^+l^-)\nu\,, \end{gathered} \tag{32}$$

where W_L and Z_L are the (mostly) SM gauge bosons, h is the SM Higgs with mass $m_h\simeq 125$ GeV, and ν represents a light neutrino of any flavor. In our analysis we also assume $m_N < m_{W_R}$, where m_N denotes collectively the pair of mass eigenvalues $(M_R^\pm)_{11}$ for the lightest heavy neutrinos, so that the RH gauge bosons $(W_R)^*$ and $(Z_R)^*$ from $N=N_{1\pm}$ decays are off-shell. We also assume for simplicity $(M_R^\pm)_{ii} > m_{W_R}$ for $i>1$ so that a single pair of RH neutrinos contributes to the signal (this second assumption is not necessary whenever

[8] This result disagrees with eq.(7) of ref. [29] which displays an explicit dependence of R_{ll} on the heavy neutrino mass M.

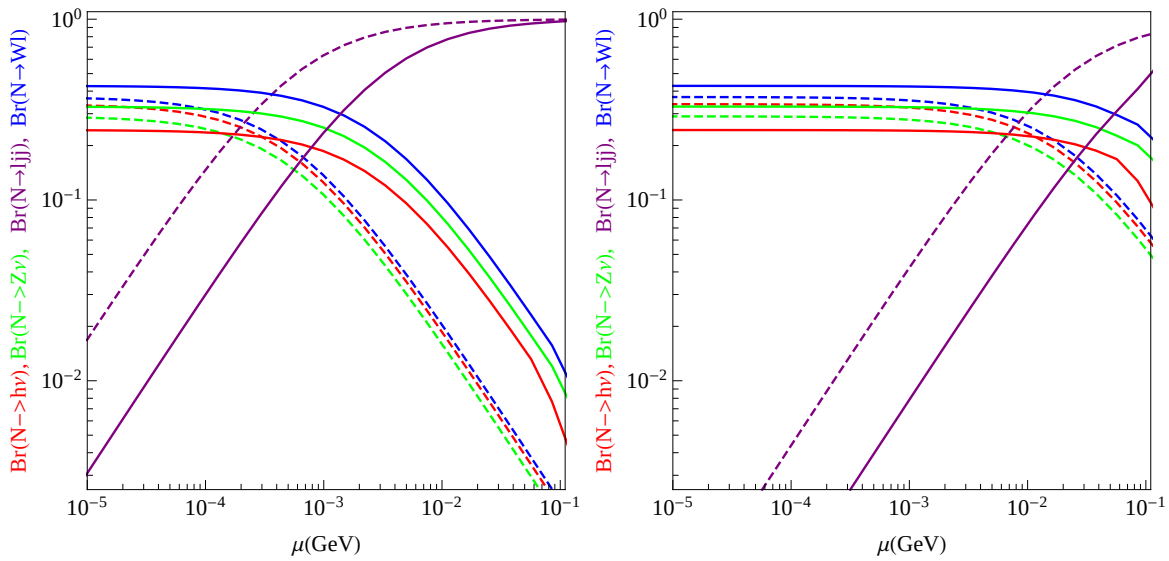

FIG. 1: Branching ratios for heavy neutrino decays as a function of μ. The blue lines are for $\Gamma(N \to W + l)$, green for $\Gamma(N \to Z + \nu)$, red for $\Gamma(N \to h^0 + \nu)$ and purple for the three-body decay $\Gamma(N \to ljj)$. Solid lines correspond to $m_N = 0.2$ TeV and dashed lines to $m_N = 0.5$ TeV. The left panel is for $m_{W_R} = 2$ TeV and the right panel for $m_{W_R} = 5$ TeV. Lepton (and quark) final states are summed over flavor indices so that there is no dependence on fermion mixings.

the different pairs of heavy neutrinos are sufficiently separated in mass so that the different invariant masses of the decay products can be reconstructed with good confidence). In the numerical analysis we have also included the decay mode $N \to (Z_R)^* + \nu$ although its branching is seesaw suppressed, and therefore largely irrelevant with respect to the other decays (see the comment below eq. (18)). In addition to the decay modes shown in eq. (32), decays into additional scalars besides the Higgs could also be possible, if they are lighter than N. This however, depends on unknown details of the scalar sector. Therefore, for definiteness we will assume that any new scalar is heavier than N so that the dominant decay modes are all listed in eq. (32).

We first present some examples of numerical results corresponding to some fixed value of m_{W_R} and of m_N. This is justified by the fact that detection of $lljj$ signals at the LHC would imply that m_{W_R} and at least one m_{N_i} will be measured. In all the plots low energy neutrino data are kept fixed at their best fit point values for a normally ordered hierarchical spectrum (no qualitative differences arise for inverted hierarchies). We start by showing results for some fixed arbitrary choice of the matrices V_R and $\mathcal{R}$ (see section II D).

Fig. 1 shows some typical values of the branching ratios for different final states as a function of the LNV parameter μ ranging within the interval $[10^{-5}, 10^{-1}]$ GeV. We have chosen the two representative values $m_N = 0.2\,\text{TeV}$ (solid lines) and $m_N = 0.5\,\text{TeV}$ (dashed lines), and two different values for the W_R mass $m_{W_R} = 2\,\text{TeV}$ (left panel) and $m_{W_R} = 5\,\text{TeV}$ (right panel). The lowest m_{W_R} value corresponds roughly to the mass of the CMS excess, while the largest one corresponds roughly to the maximum m_{W_R} that the LHC can

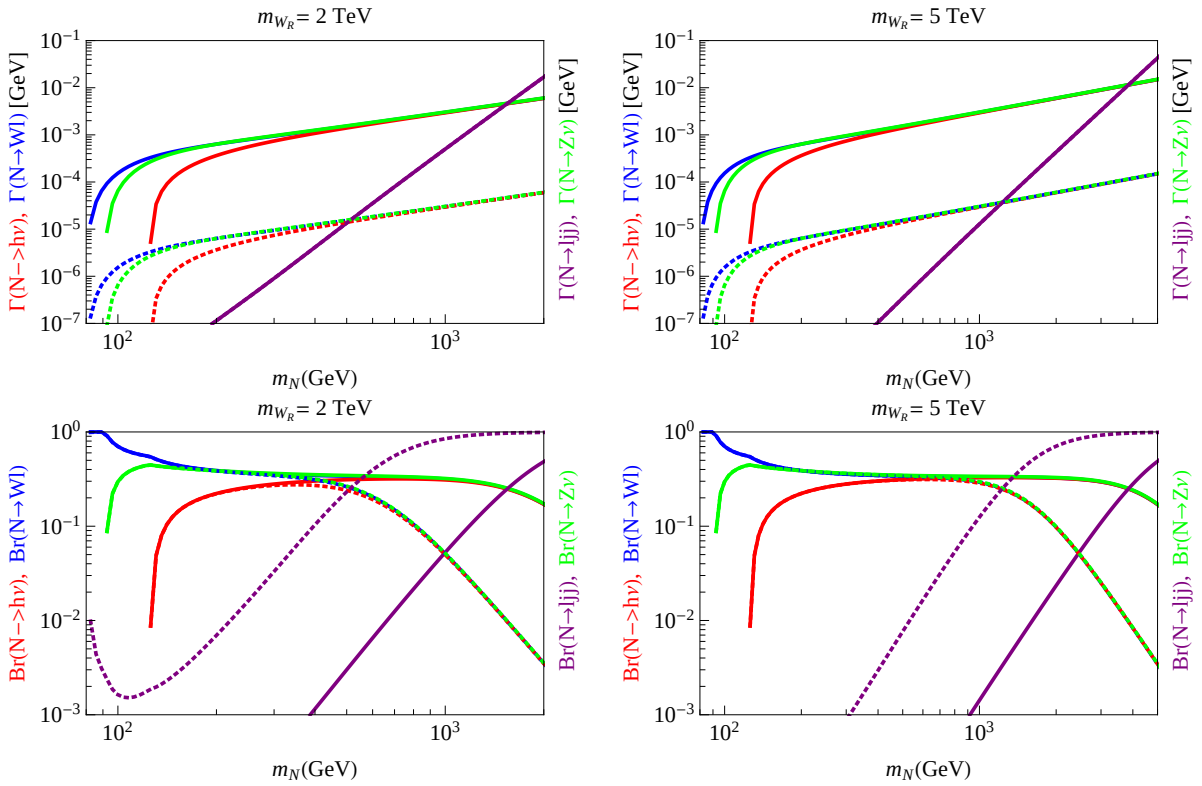

FIG. 2: Partial decay widths in GeV (top panel) and branching ratios (bottom panel) for N decays. The blue, green and red lines are respectively for $\Gamma(N \to W + l)$, $\Gamma(N \to Z + \nu)$ and $\Gamma(N \to h^0 + \nu)$ while the purple lines are for the three-body decay $\Gamma(N \to ljj)$. Solid lines correspond to $\mu = 10^{-5}\,\text{GeV}$ and dashed lines to $\mu = 10^{-4}\,\text{GeV}$. Left panels correspond to $m_{W_R} = 2\,\text{TeV}$ and right panels to $m_{W_R} = 5\,\text{TeV}$.

probe in the next few years of running. In the final states we sum over the different quark and lepton generations, so that the results are independent of neutrino mixing. For small values of μ, decays to SM gauge bosons dominate the decay rates. The branching ratios for $N \to W_R^* + l^\mp \to l^\mp jj$ and for decays to SM gauge bosons become similar for intermediate values of μ, the detailed ranges in which this occurs depend, however, rather strongly on the values of m_N and of m_{W_R}. For large values of μ three body decays become dominant. The qualitative behavior shown in fig. 1 can be understood from the equations presented in the previous section. In the inverse seesaw, the light neutrino masses are given by eq. (6). The equation contains the three matrices m_D, M_R and μ as free parameters. Keeping fixed the light neutrino masses at values in agreement with the experimental data and for fixed values of M_R, a scaling $m_D \propto 1/\sqrt{\mu}$ is obtained. Since all the couplings of the heavy neutrinos to SM gauge bosons are proportional to m_D (see the equations in section II C) decays to SM gauge bosons dominate when μ is small.

Fig. 2 shows the partial widths and branching ratios for N decays as a function of m_N for the two values $\mu = 10^{-5}\,\text{GeV}$ (solid lines) and $\mu = 10^{-4}\,\text{GeV}$ (dashed lines). Typical widths are in the range of $\Gamma \simeq [10^{-7}, 10^{-2}]$ GeV, much too small to be directly measured at

the LHC, and too large to produce a displaced vertex. For small values of m_N, $N \to W_L l^\pm$ decays dominate the other two-body decays. However, it is important to notice that for $m_N \gg m_h$ the branching ratios of N decays to W_L, Z_L and h summed over light flavors become all equal. This can allow to infer the branching ratio for N decays to $W_L + Z_L + h$ from the measurement of $\mathrm{Br}(N \to W^\pm + \sum_\alpha l_\alpha^\mp)$ alone.

Note also that the W_L gauge bosons decay to jets with a branching ratio of about $2/3 < 1$, and that Z_L and h do not lead to ljj final states. This implies a reduction in the number of expected $lljj$ events. In the extreme case of very small μ and for $m_N \gg m_h$, when the decays into SM bosons dominates, only 1/9 of the total number of decays are into $lljj$ final states occurring mainly via the $N \to W_L + l \to ljj$ decay chain. Let us recall that experimental estimates are instead based on the assumption that the only decay channel is $N \to W_R^* l^\pm$, implying that 100% of the decays correspond to ljj final states. Therefore, we can expect that, within the present framework, the lower limit on m_{W_R} should be somewhat looser than the one quoted by the LHC collaborations. Let us also note that since W_L's are produced on-shell, for $N \to W_L + l \to ljj$ decays, the invariant mass of the jets should be peaked in correspondence to m_{W_L}. Thus it should be possible to separate kinematically these events from the off-shell W_R events. Such a measurement could be important to establish large "heavy-light" mixing in the neutrino sector, that is a general prediction of the inverse seesaw model. Finally, the fact that in the inverse seesaw models decays to SM bosons can dominate in a wide region of parameter space is again apparent also from fig. 2.

Up to now we have kept the values of the entries of the V_R and $\mathcal{R}$ matrices in the parametrization given in eq. (22) fixed at some arbitrary constant values. We recall that V_R is a unitary matrix with three angles and three phases, while $\mathcal{R}$ is complex orthogonal and can be defined in the usual way in terms of sin and cos of three complex angles ζ_i. For our numerical scan, we parametrize these angles as:

$$\zeta_i = \kappa \cdot e^{2i\pi\, x_i}, \tag{33}$$

with x_i a randomly generated real number $\in [0, 1]$, and $\kappa \in [0, \kappa_{\max}]$. The upper limit $\kappa_{\max}$ represents a measure of how much fine tuning is allowed in the parametrization eq. (23) in order to allow for particularly large values of m_D (or alternatively of the Yukawa couplings generating m_D) while still respecting all the constraints from low energy neutrino data. For $\kappa_{\max} \lesssim 1$ there is no fine tuning: all the tree-level formulas presented above remain valid and in particular loop corrections to neutrino masses and mixing angles remain at the level of few percent. However, for $\kappa_{\max} \gtrsim 2 - 3$, similarly large values of κ become possible and the corresponding results would be highly questionable, since the tree-level approximation starts to break down and in particular, when loop corrections are taken into account, some low energy neutrino parameters might well drop out the experimentally allowed range. We have then plotted the results in fig. (3) adopting the educated choice $\kappa_{\max} = 1$.

In the left panel of fig. 3 we depict R_{ll} versus $\Delta M/\Gamma$ for some arbitrary value of the heavy neutrino mass, scanning randomly over the entries in V_R and $\mathcal{R}$. We see that for ΔM larger than a few times Γ, R_{ll} approaches rapidly the Majorana limit $R_{ll} = 1$. This result is independent of the absolute mass scale of the heavy neutrinos.

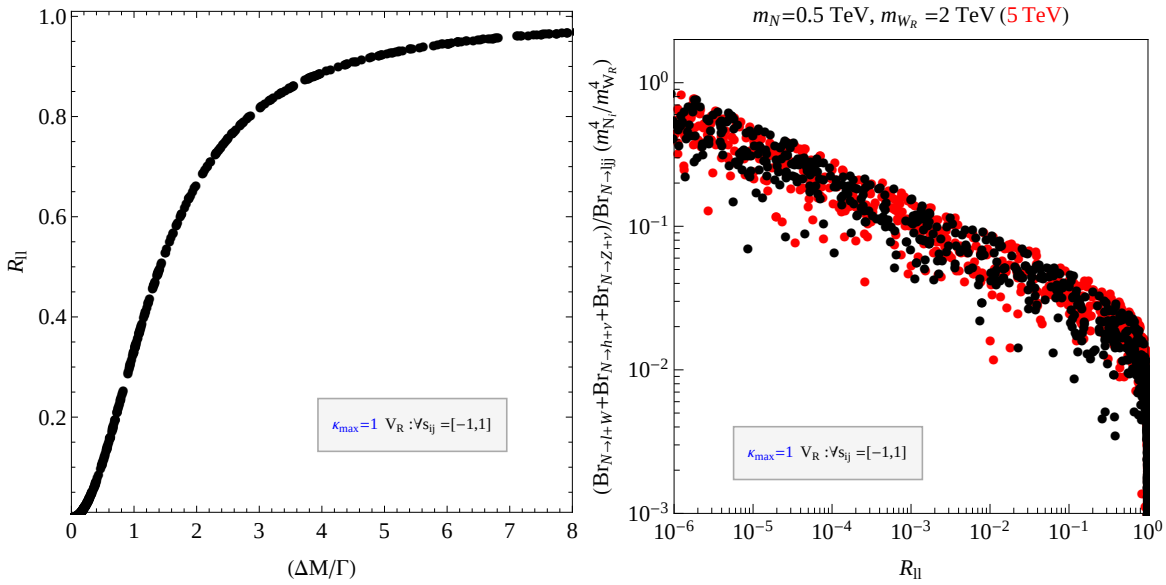

FIG. 3: Left panel: the SS to OS ratio R_{ll} versus $\Delta M/\Gamma$. Right panel: the sum of the branching ratios of N decays to SM bosons divided by the branching ratio to ljj, versus R_{ll}. The numerator has been rescaled by $(m_N/m_{W_R})^4$ to compensate for the W_R-propagator suppression in the denominator. Black points are for $m_{W_R} = 2$ TeV, red points for $m_{W_R} = 5$ TeV, and $m_N = 0.5\,\text{TeV}$.

As we have already noticed, the expected widths for the heavy neutrino decays are too small to be directly measured at the LHC (see fig. 2). However, the ratio of two-body versus three-body N decays can be measurable. At fixed values of m_N and m_{W_R} this ratio is controlled by the value of μ, which also fixes the mass splitting of the quasi-Dirac neutrino pair, therefore we can expect a correlation between the ratio of two body versus three body N decays, and R_{ll}. This is shown in the right panel in fig. (3) where this ratio is plotted versus R_{ll} (summed over lepton flavors). The sum of the two body decays in the numerator of the ratio (y-axis in the right panel), has been rescaled by $(m_N/m_{W_R})^4$ to compensate for the W_R-propagator suppression for the three body decay. This renders the correlation between the two observables nearly independent of the values of the W_R and N masses. As the figure shows, if a large value $R_{ll} \sim 1$ is measured, the present scenario predicts that the rate for decays into SM bosons should be smaller than a few percent of the rate for three body decays times $(m_N/m_{W_R})^4$. On the other hand, if a small value $R_{ll} \lesssim 10^{-2}$ is measured (or an upper bound of the same order is set), the prediction is that a sizeable fraction of RH neutrino decays should proceed via on-shell SM bosons. Note that this correlation does not depend on the type of light neutrino spectrum (normal versus inverted hierarchy). Thus, the inverse seesaw not only allows for generic values $R_{ll} < 1$, but it also implies a testable correlation between R_{ll} and the RH neutrino decay modes.

As we have already said, the results depicted in the plots have been obtained by summing over the the final state lepton flavors. However, given that the mixing matrices controlling the flavor composition of the dilepton final states are in principle generic, different flavor final

states such as μejj can naturally occur with large branching ratios, while respecting the full set of low energy constraints (we have checked that numerically generated dilepton samples do not show suppressions of different flavor dilepton events). Thus, we stress again that SS and OS dilepton events of different flavors should be included as a potential contribution to the signal and, most importantly, they should not be used as an estimate of the backgrounds in experimental analyses. In the attempt of scrutinizing further lepton flavor violating (LFV) effects in the inverse seesaw scenario, we have also calculated branching ratios for low energy LFV processes, the most relevant of which is $\mathrm{Br}(\mu \to e\gamma)$. We have found that $\mathrm{Br}(\mu \to e\gamma)$ can provide additional relevant constraints only for very small values of μ ($\mu \ll 10^{-6}$ GeV), which corresponds to the regime in which the pure Dirac limit is approached and $R_{ll} \approx 0$ is expected.

All in all, the main conclusion of this section is that LR models equipped with an inverse seesaw mechanism for the light neutrino masses naturally yield pairs of quasi-Dirac RH neutrinos. In the specific region of parameter space corresponding to $\Delta M \approx \Gamma$, the ratio R_{ll} can have any value within the range [0,1]. Moreover, this value correlates in a specific way with the value of the ratio between two-body and three-body RH neutrino decays, and gross violations of this prediction would disfavor the scenario, and possibly rule it out.

V. SUMMARY

In this paper we have discussed signals of LNV that could originate in scenarios with quasi-Dirac neutrinos, that can be defined as a pair of Majorana neutrinos for which a mass splitting much smaller than their average mass is induced by small LNV terms. In particular, we have focused on the ratio of same-sign to opposite-sign dilepton events R_{ll}, which is the most promising LNV observable for experimental searches at the LHC. It is well known that if the dilepton events originate from production/decays of heavy Majorana neutrinos, then $R_{ll} = 1$ is expected. We have shown that in the quasi-Dirac case, in the regime in which the mass splitting ΔM between the pair of heavy RH neutrino resonances becomes of the order of their widths, any value within the interval $R_{ll} \in [0, 1]$ is possible, and $R_{ll} = 0$ is approached in the limit $\Delta M/\Gamma \to 0$ which defines the pure Dirac limit of the quasi-Dirac neutrino pair. It is then clear that an experimental result $R_{ll} < 1 (\neq 0)$ could provide valuable information about the mechanism of generation of the light neutrino masses.

We stress that our main result on R_{ll} does not depend on the particular model realization of the quasi-Dirac neutrino scenario (other features, as for example the total event rate for heavy neutrino production, obviously do depend on the specific model). For definiteness we have carried out our discussion in the framework of a LR symmetric model equipped with an inverse seesaw mechanism, since this setup appears to be of prominent experimental interest in view of the ongoing searches for signals of LNV and of RH neutrinos at the LHC. In discussing the LHC phenomenology, we have pointed out that specific values of $R_{ll} \neq 0, 1$ can be correlated with special features of observables in the decay modes of the

heavy neutrinos, and this correlation can help to test the scenario. Last but not least, in developing our analysis we have introduced a new parametrization of the inverse seesaw which allows to scan the parameter space of the fundamental theory while automatically respecting all the phenomenological constraints of the low energy effective theory. The use of this parametrization has proven to be very convenient in carrying out our numerical study.

Acknowledgments

We thank R.N. Mohapatra and P. S. Bhupal Dev for discussion about their results. The work of E.N. is supported in part from the research grant "Theoretical Astroparticle Physics" number 2012CPPYP7 under the program PRIN 2012 funded by the Italian "Ministero dell' Istruzione, Università e della Ricerca" (MIUR) and from the INFN "Iniziativa Specifica" Theoretical Astroparticle Physics (TAsP-LNF). This work was supported by the Spanish grants FPA2014-58183-P, Multidark CSD2009-00064 and SEV-2014-0398 (from the *Ministerio de Economa y Competitividad*), as well as PROMETEOII/2014/084 (from the *Generalitat Valenciana*).

---

[1] I. Avignone, Frank T., S. R. Elliott, and J. Engel, Rev.Mod.Phys. **80**, 481 (2008), arXiv:0708.1033.

[2] F. F. Deppisch, M. Hirsch, and H. Päs, J.Phys. **G39**, 124007 (2012), arXiv:1208.0727.

[3] W.-Y. Keung and G. Senjanovic, Phys.Rev.Lett. **50**, 1427 (1983).

[4] J. C. Pati and A. Salam, Phys.Rev. **D10**, 275 (1974).

[5] R. Mohapatra and J. C. Pati, Phys.Rev. **D11**, 2558 (1975).

[6] R. N. Mohapatra and G. Senjanovic, Phys. Rev. **D23**, 165 (1981).

[7] J. Helo, M. Hirsch, H. Päs, and S. Kovalenko, Phys.Rev. **D88**, 073011 (2013), arXiv:1307.4849.

[8] M. Fukugita and T. Yanagida, Phys. Lett. **B174**, 45 (1986).

[9] W. Buchmuller, P. Di Bari, and M. Plumacher, Annals Phys. **315**, 305 (2005), arXiv:hep-ph/0401240.

[10] S. Davidson, E. Nardi, and Y. Nir, Phys. Rept. **466**, 105 (2008), arXiv:0802.2962.

[11] C. S. Fong, E. Nardi, and A. Riotto, Adv. High Energy Phys. **2012**, 158303 (2012), arXiv:1301.3062.

[12] R. N. Mohapatra and J. W. F. Valle, Phys. Rev. **D34**, 1642 (1986).

[13] E. K. Akhmedov, M. Lindner, E. Schnapka, and J. W. F. Valle, Phys. Rev. **D53**, 2752 (1996), arXiv:hep-ph/9509255.

[14] E. K. Akhmedov, M. Lindner, E. Schnapka, and J. W. F. Valle, Phys. Lett. **B368**, 270 (1996), arXiv:hep-ph/9507275.

[15] S. Bray, J. S. Lee and A. Pilaftsis, Nucl. Phys. B **786**, 95 (2007) [hep-ph/0702294 [HEP-PH]].

[16] J. Kersten and A. Y. Smirnov, Phys. Rev. D **76**, 073005 (2007) [arXiv:0705.3221 [hep-ph]].

[17] ATLAS Collaboration, G. Aad et al., Eur.Phys.J. **C72**, 2056 (2012), arXiv:1203.5420.

[18] ATLAS, G. Aad et al., JHEP **07**, 162 (2015), arXiv:1506.06020.

[19] CMS Collaboration, report CMS-PAS-EXO-12-017 (2012).

[20] CMS, V. Khachatryan et al., Eur. Phys. J. **C74**, 3149 (2014), arXiv:1407.3683.

[21] See articles referring to [20]: http://inspirehep.net/record/1306295/citations

[22] F. F. Deppisch, T. E. Gonzalo, S. Patra, N. Sahu and U. Sarkar, Phys. Rev. D **90**, no. 5, 053014 (2014) doi:10.1103/PhysRevD.90.053014 [arXiv:1407.5384 [hep-ph]].

[23] M. Heikinheimo, M. Raidal and C. Spethmann, Eur. Phys. J. C **74**, no. 10, 3107 (2014) doi:10.1140/epjc/s10052-014-3107-9 [arXiv:1407.6908 [hep-ph]].

[24] B. A. Dobrescu and Z. Liu, Phys. Rev. Lett. **115**, no. 21, 211802 (2015) doi:10.1103/PhysRevLett.115.211802 [arXiv:1506.06736 [hep-ph]].

[25] J. Brehmer, J. Hewett, J. Kopp, T. Rizzo and J. Tattersall, JHEP **1510**, 182 (2015) doi:10.1007/JHEP10(2015)182 [arXiv:1507.00013 [hep-ph]].

[26] K. Cheung, W. Y. Keung, P. Y. Tseng and T. C. Yuan, Phys. Lett. B **751**, 188 (2015) doi:10.1016/j.physletb.2015.10.029 [arXiv:1506.06064 [hep-ph]].

[27] F. F. Deppisch, L. Graf, S. Kulkarni, S. Patra, W. Rodejohann, N. Sahu and U. Sarkar, Phys. Rev. D **93**, no. 1, 013011 (2016) doi:10.1103/PhysRevD.93.013011 [arXiv:1508.05940 [hep-ph]].

[28] B. Allanach, S. Biswas, S. Mondal and M. Mitra, Phys. Rev. D **91**, no. 1, 011702 (2015) doi:10.1103/PhysRevD.91.011702 [arXiv:1408.5439 [hep-ph]].

[29] P. S. Bhupal Dev and R. N. Mohapatra, Phys. Rev. Lett. **115**, 181803 (2015), arXiv:1508.02277.

[30] F. F. Deppisch, P. S. Bhupal Dev and A. Pilaftsis, New J. Phys. **17**, no. 7, 075019 (2015)

[31] D. Forero, M. Tortola, and J. Valle, Phys.Rev. **D90**, 093006 (2014), arXiv:1405.7540.

[32] J. Casas and A. Ibarra, Nucl.Phys. **B618**, 171 (2001), arXiv:hep-ph/0103065.

[33] Y. Nir, Conf. Proc. **C9207131**, 81 (1992).